

**Paleoearthquake History of the North Anatolian Fault, Western Turkey: An Investigation  
into the Nature of Earthquake Recurrence as Revealed by Precise Stratigraphic and  
Historical Records**

Final Technical Report  
Award No. 00HQGR0034

Thomas Rockwell, P.I.  
Geological Sciences  
San Diego State University  
San Diego, CA 92182  
[Trockwel@geology.sdsu.edu](mailto:Trockwel@geology.sdsu.edu)

(With Gordon Seitz, Rob Langridge, Aykut Barka, Aron Meltzner, Yann Klinger, Daniel Ragona, Mustapha Meghrouri, Matthieu Ferry)



240.9(680)

R 624P

2002

## **Paleoearthquake History of the North Anatolian Fault, Western Turkey: An Investigation into the Nature of Earthquake Recurrence as Revealed by Precise Stratigraphic and Historical Records**

### **Introduction**

Information on the size and timing of past earthquakes is important in understanding fault behavior, a key element in forecasting future seismic activity (Sieh, 1996). The North Anatolian fault (NAF) in Turkey (Barka, 1992)(Figure 1) is an ideal candidate for understanding fault behavior over multiple earthquake cycles because there is a long and excellent historical record of large earthquakes going back over 2000 years (Ambraseys and Finkel, 1987, 1991, 1995) (Figure 2). Furthermore, Like the San Andreas fault of southern California, it is a fast-moving fault (~23 mm/yr, Straub and Kahle, 1995; Straub, 1996; Reilinger et al., 1997) resulting in many earthquakes for each fault segment during this long historical period. It is also fairly segmented, and most of the fault zone has ruptured this past century. Thus, there is the opportunity to collect information on the patterns of large earthquake generation over many earthquake cycles, as well as their sizes and repeatability. In this paper, we present new results that further quantify the earthquake history of the North Anatolian fault both east and west of the Marmara Sea.

To the west near the Gulf of Saros, we continued paleoseismic investigations and resolved slip for the past two large earthquakes that struck the Galipoli region in 1766 and 1912. The Saros study area lies within the township of Kavakkoy (Figures 1 and 2) close to where we completed earlier studies (Rockwell et al., 2001). We had determined that four surface ruptures have occurred near where the fault passes offshore into the Gulf of Saros during the past 1100 years or so. However, the dating was insufficiently precise to confidently resolve which of the historical events these were. In this new study, we focused on a young (post-1600 A.D.) stream channel that crosses the fault at a high angle and is offset by the fault across a narrow zone. Twenty-two trenches were excavated at this new site to resolve total slip on the channel and to further constrain the timing of ruptures that produced the slip.

East of the Marmara Sea, we continued efforts between Izmit and Lake Sapanca that we had begun prior to the August 1999 Izmit earthquake. Specifically, we excavated new trenches within and adjacent to an Ottoman canal, dated at ca 1591 from historical data (Finkel and Barka,

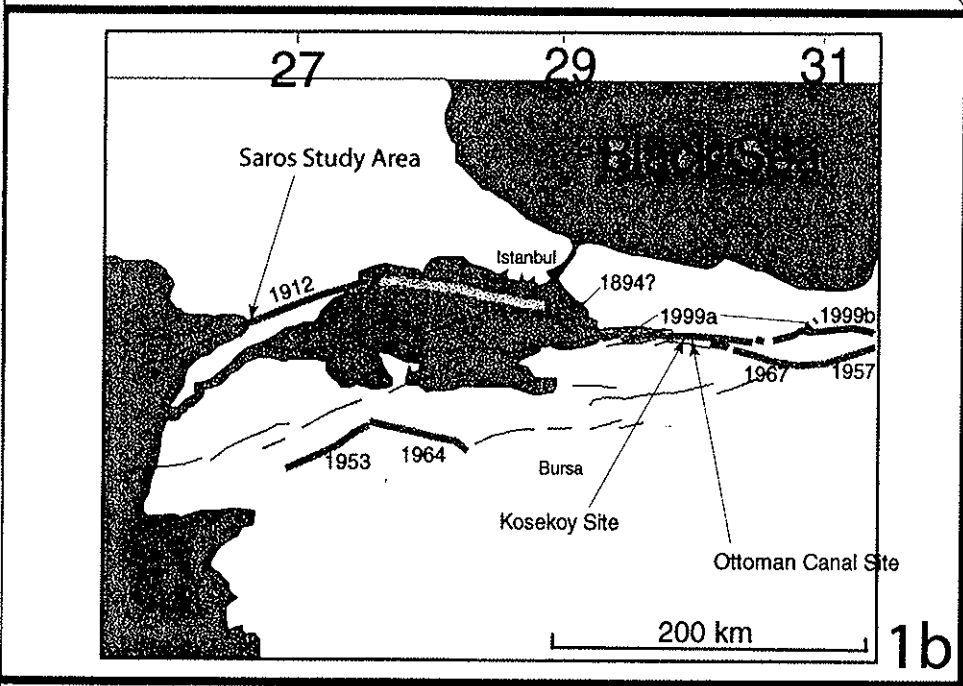
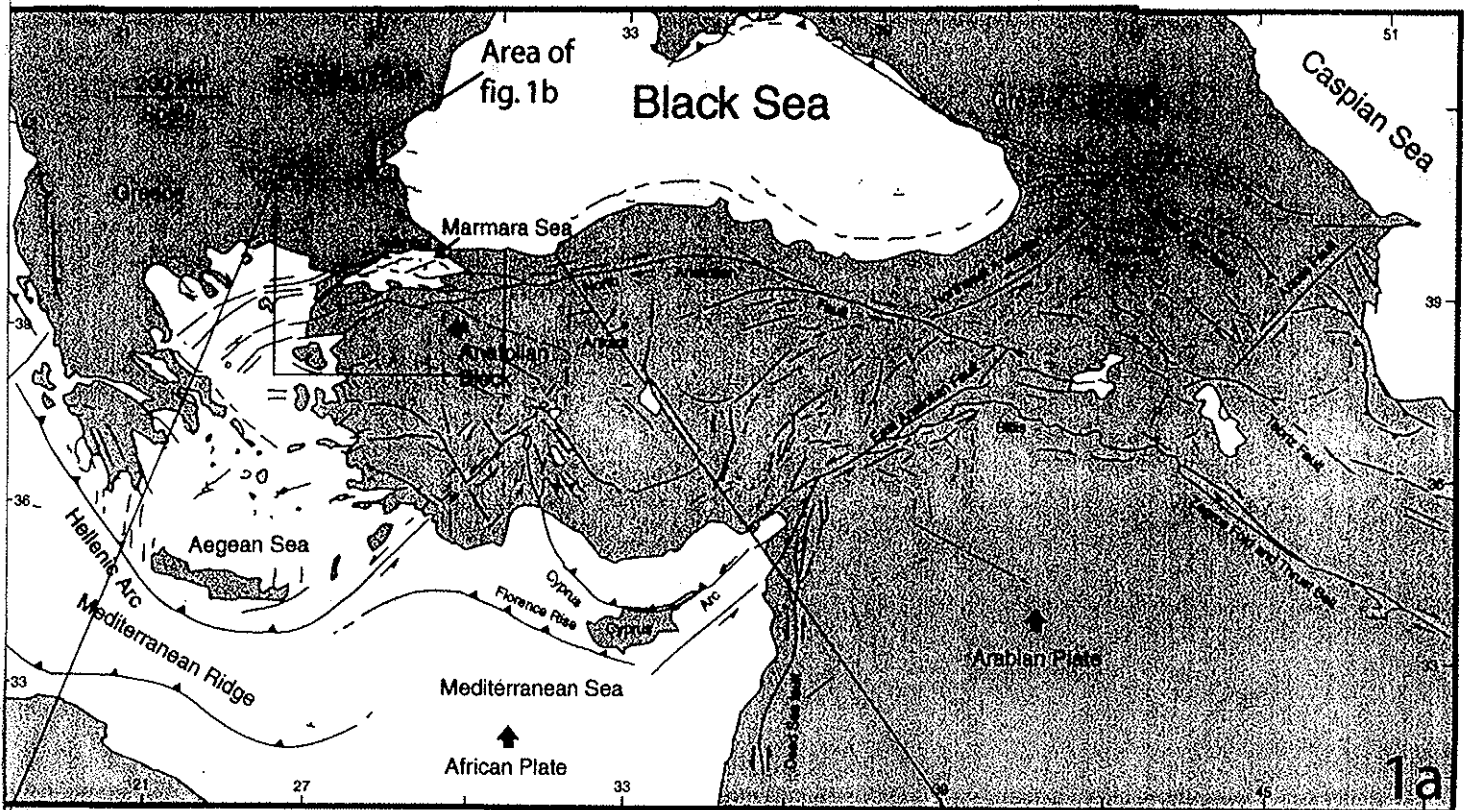
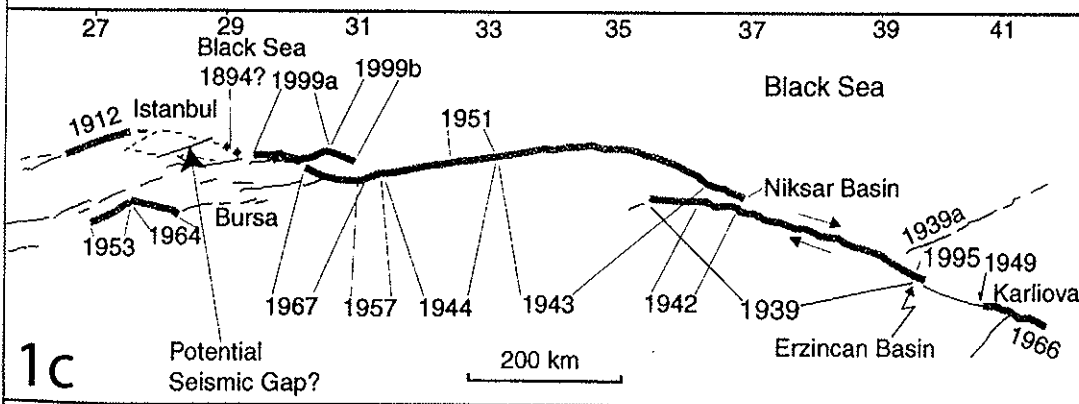


Figure 1. a) Generalized tectonic map of the Middle East. The North Anatolian fault bounds the Anatolian block on the north, allowing the westward escape of Anatolia. The box shows the area of detail in b), showing the specific study areas along the fault. Note the historical ruptures during the past century or so. The Marmara segment has not ruptured since 1766. c) large ( $M > 7$ ) 20th century earthquakes along the North Anatolian fault. Note the generally westward progression of many of these events after 1939.



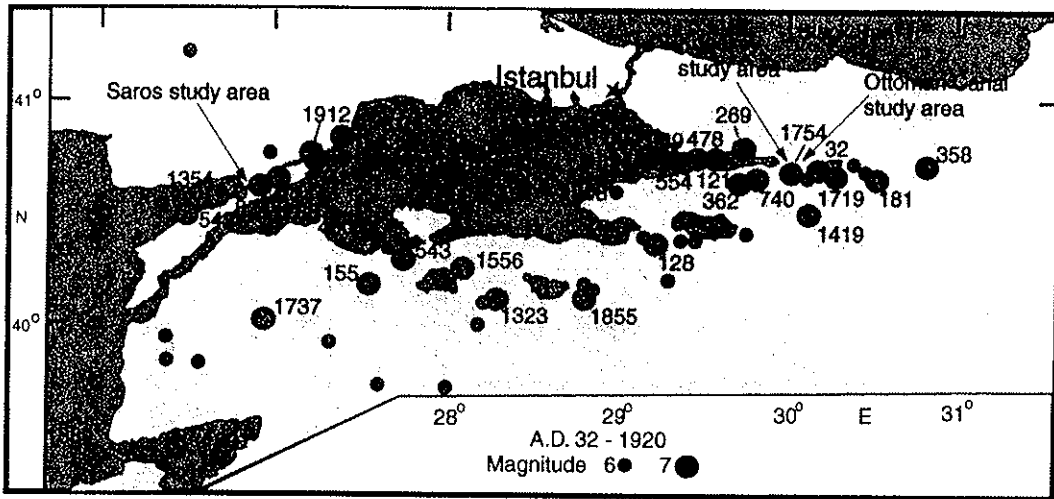


Figure 2. Map showing historical moderately large to large earthquakes along the North Anatolian fault zone during the past 2000 years.

1999; C. Finkel, personal communication) to resolve the history of surface ruptures for the past 400 years east of Izmit Bay.

Each of these studies bear on the impending seismic hazard to Istanbul, which lies close to the NAF beneath the Marmara Sea. Our observations support the contention that the NAF near Istanbul should be close to failure based on the distribution and size of earthquakes during the past 400 years, and that the recent earthquakes to the east (Izmit and Duzce events in 1999) have further loaded the fault segments beneath the Marmara Sea (Parsons et al., 2000).

### **The Saros Site**

Earlier paleoseismic results at Kavakkoy in the Galipoli Peninsular region near the Gulf of Saros indicate that four earthquakes have ruptured the surface in that area during the past 1000-1200 years, and that two of these post-date a sand channel dated to younger than the fourteenth century. One of these is almost certainly the surface rupture of the 1912 M7.4 earthquake, which was photographed east of our site towards the Marmara side of the peninsula (Ambraseys and Finkel, 1987a).

We analyzed low altitude stereo photography of the fault along the westernmost few kilometers before it passes offshore into the Gulf (figure 3), to search for the best sites to resolve slip. In the area of T-1 from the Rockwell et al. (2001) study, we recognized the presence of an abandoned tributary channel to the Kavak River that crosses the fault at a high angle, and is the likely source for the sand exposed in our original T-1 trench. At the fault, sediments in the abandoned channel appear in the aerial photography to splay out southward across the fault, indicating that a low scarp is present where the fault crosses the channel. We hoped to expose buried elements of the channel system and resolve slip on buried piercing points, to better constrain the age of these channel deposits, and to further resolve the number of earthquakes that affect the buried sand channel sediments. Towards this aim, we focused our efforts on the margins of the channel and excavated a total of 26 trenches across and parallel to the fault (Figures 3 and 4). The central part of the channel is now occupied by an elevated highway and berm and was no longer available for study.

Several of the trenches that contained important information on past surface ruptures were logged in detail on photographs and later entered into the computer in rectified form. Many of the trenches, however, were excavated for the sole purpose of tracing out the distribution of

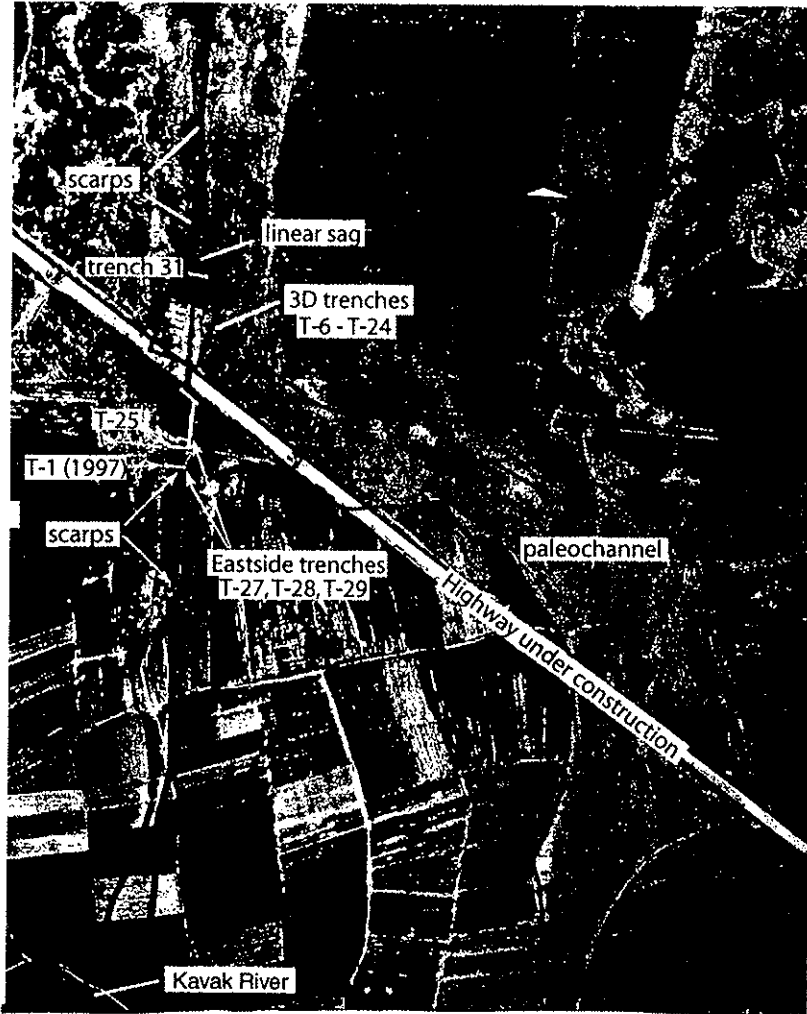


Figure 3. Photomap of the Saros trench sites. Note the paleochannel that flowed at a high angle across the fault.

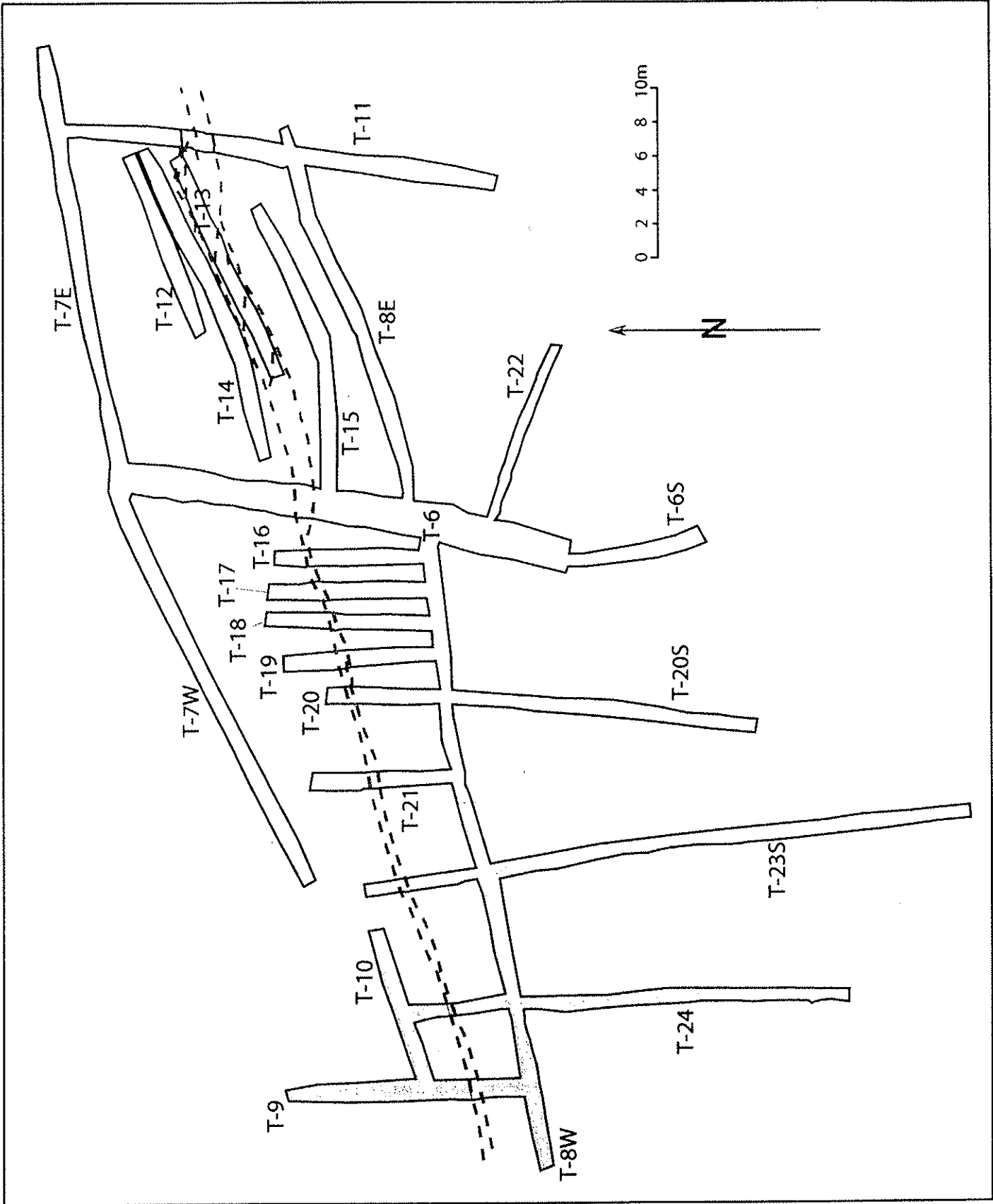


Figure 4. Map of trenches and faults in the area of detailed 3D work.

the distinctive well-sorted sand body, and data from these trenches was collected on the thickness of the sand but they were not logged in detail. All trench locations, including sand thickness control points, were surveyed with a Wild TC-2000 total station, and all have the same reference elevations established by surveyed horizontal string lines. Further, all critical contacts, relevant stratigraphic pinch outs, etc. were surveyed to precisely locate them in 3D space.

Site Stratigraphy - All of the trenches exposed a similar succession of young sediments, with or without a distinctive clean, well-sorted channelized sand. Figure 5 is a detailed log of the east face of trench T-6, and shows the typical stratigraphy of the site, with unit 200 being the distinctive sand that is only exposed on the south side of the fault in this trench. This sand is the same as unit 3 described in trench T-1 by Rockwell et al. (2001), and was also exposed in new trenches near the original T-1 on the east side of the highway (Figures 6 and 7). We use the lateral extent of this distinctive sand to constrain cumulative slip on the most recent surface ruptures. In this section, we briefly describe each of the primary units and the associated radiometric control on their ages.

We identified several primary units, along with dozens of secondary contacts, within the section exposed in the trenches. Units are given numeric designations ranging from 10 (topsoil; youngest) to 350 (oldest). Within a given trench, correlation of units both laterally along the trench and from wall to wall is fairly certain, and is based on the character of several distinctive strata contained within the section. Conversely, unit designations in the upper section of T-6 may be generally similar to those in the trenches east of the highway, but their correlation is by inference because we did not connect trenches between these sites (because of the highway). Thus, unit 100 at T-6 may not be exactly the same stratum as unit 100 in the East Saros trenches, although it is similar and falls in the same part of the section. The only unit for which we feel confident to be the same in all exposures is the distinctive well-sorted sand of unit 200. Even this unit, however, may have some variance in age across the overall study area (few decades or less?) as the sand in the eastern group of trenches was associated with the main channel deposits whereas the sand at T-6 was deposited by a secondary tributary overflow channel, as discussed later.

The deepest (oldest) stratum, unit 350, was exposed at a depth of about 1.5 m on the north side of the fault in T-6, just above the water table. Units 210 through 350 are generally

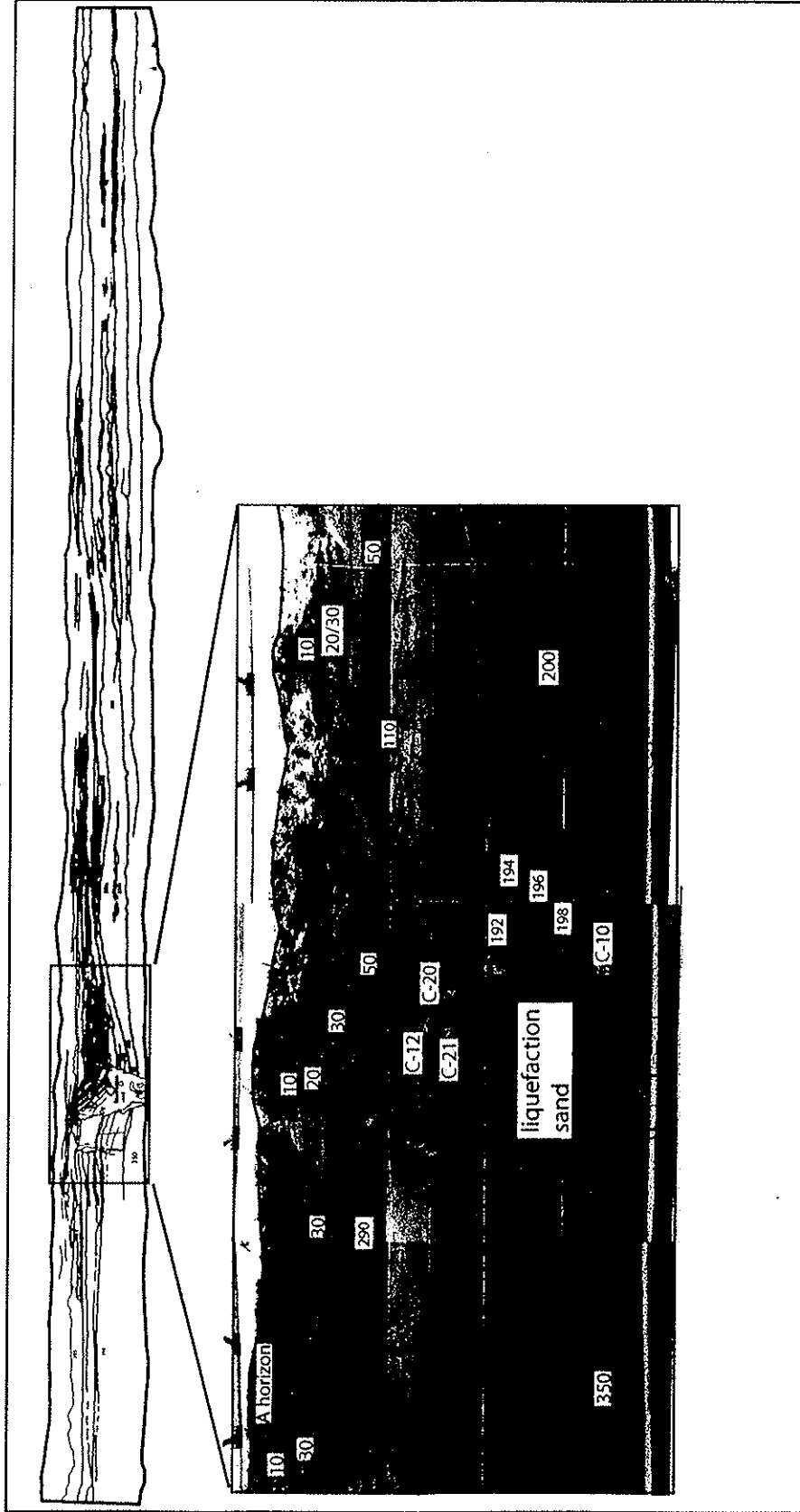


Figure 5. Log of the east face of trench T-6. Units are described in the text.

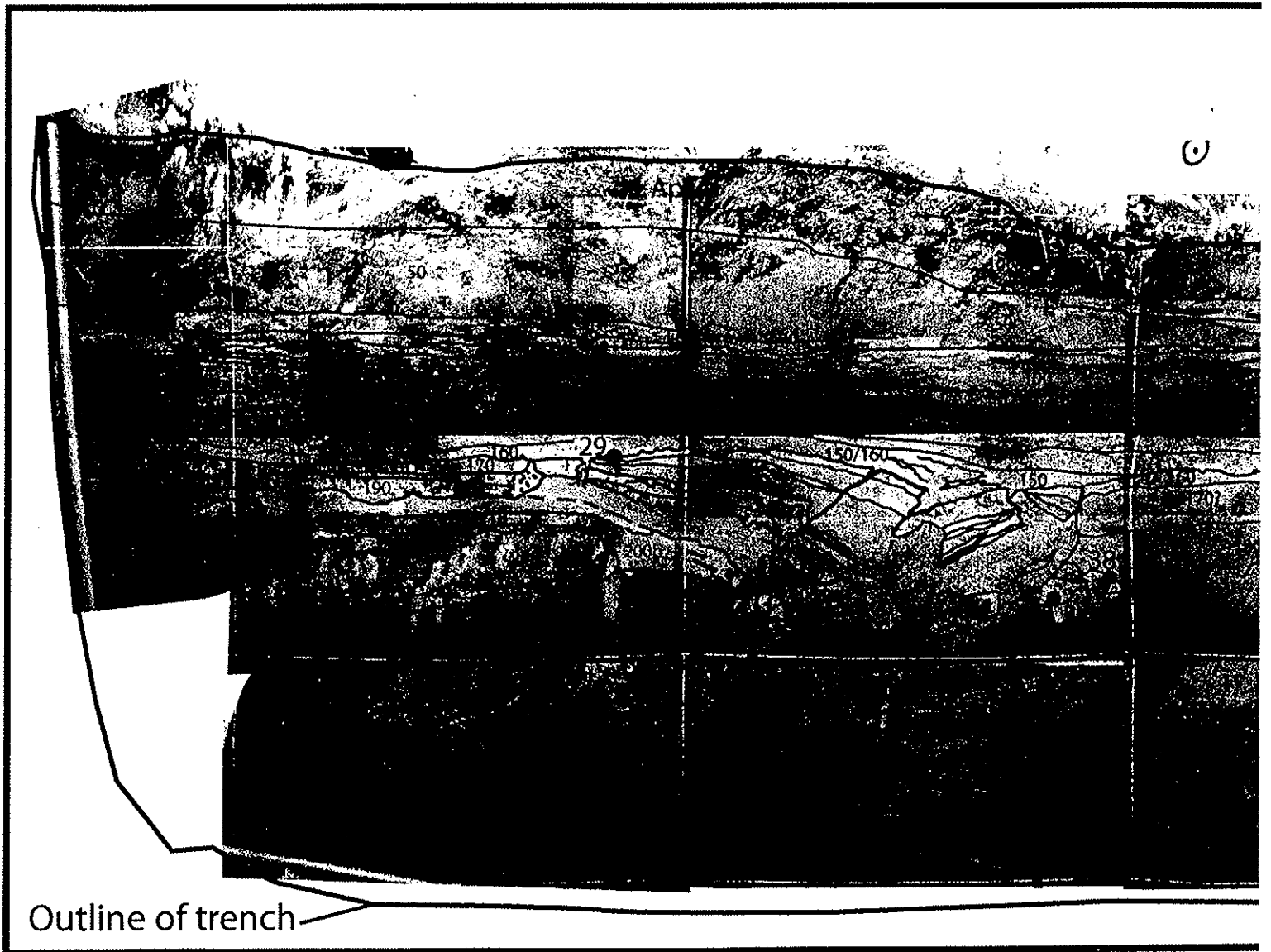


Figure 6. Log of the east face of trench T-25, west side of the highway. Units are described in the text.

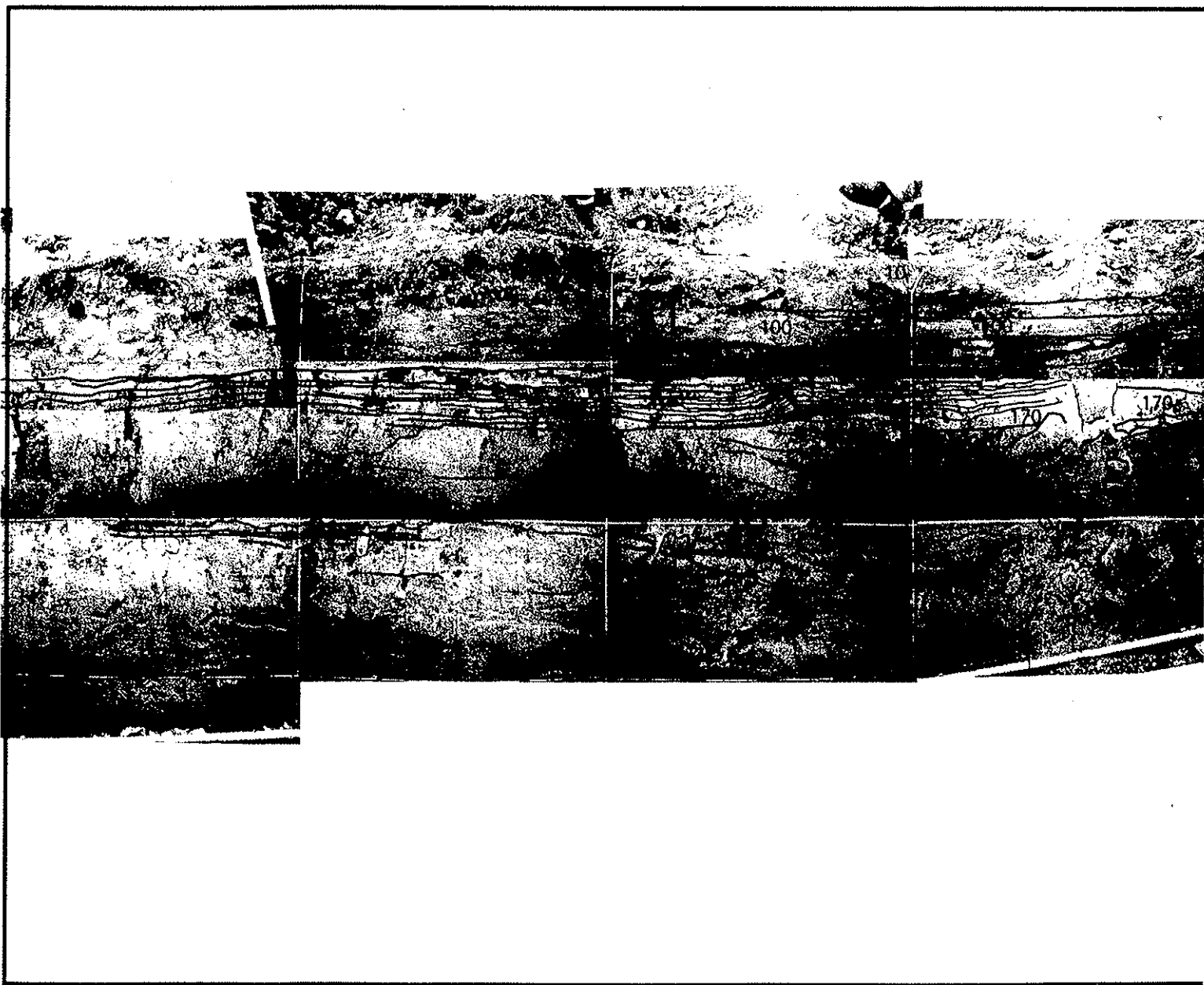


Figure 7. Log of the west face of trench T-25, east side of the highway. Units are described in the text.

fine-grained silt and clay strata interpreted as a succession of over-bank deposits to the main Kavak River. The only age control for this part of the section is from two dates on a sample split (T6-6) from near the base of this section that yielded consistent calibrated ages of about 1-2 centuries BC. As this sample could have been re-worked or have been resident in the system for some period of time, this represents a maximum age for this part of the section.

Unit 200 is the distinctive well-sorted sand that we use to constrain lateral slip, and is therefore of considerable interest. The sand is channelized and its distribution is locally restricted or absent. In our analysis of the aerial photography (figure 3), we interpret a tributary or overflow channel to the Kavak River as the primary source for this sand. Within this tributary system, we exposed the sand in most of the trenches and can make some general observations about its extent.

East of the highway, the sand fills a major, broad channel, and the sand is locally over a meter thick. We excavated a trench parallel to the fault between T25 and the highway, and the sand locally extended to below the depth of the 2-m-deep trench. This was an exploratory trench to determine the character of the sand and was not logged in detail because of safety constraints. Nevertheless, it was clear to us that the primary fluvial channel lies east of the highway, and our trench 25 lies near the margin of this system. Trench T-1 of Rockwell et al. (2001), which lies within 10 m to the east of T25, also exposed this sand unit (unit 3 in their trench log).

West of the highway, unit 200 is substantially more restricted in its aerial extent. North of the fault, the well-sorted sand is restricted to a narrow and shallow (<20 cm) "feeder" channel that flowed from north to south across the fault. South of the fault, the sand thickens dramatically and locally reaches over 40 cm in thickness. We collected observations on the sand thickness in all exposures to provide a basis for developing an isopach map of the sand (Figure 8). We collected these observations at a maximum spacing of 50 cm and tied all measurements to a common, surveyed system of horizontal string lines. We also measured the absolute height of the top and bottom of the sand relative to the string datum to provide a complete spatial reference. These data are presented later to resolve slip on the channel fill of unit 200.

The age of unit 200 is well constrained to be younger than A.D. 1655. We dated several samples from this unit, along with those above and below it, and use the youngest date to constrain its maximum age. All of the samples constrain the sand to the past 500 years, but sample T6-43, recovered from stratified alluvium within the channel, can be no older than A.D.

CAMS #	Sample Name	Trench Exposure	Notes	Unit	$\delta^{13}C$	fraction Modern	$\pm$	D14C	$\pm$	14C age	$\pm$	Calibrated Age Range (2 $\sigma$ )
Kavakkoy and Saros												
67291	K-T14-48	Proxy to T6		92	-25	0.9556	0.0048	-44.4	4.8	360	50	AD 1451-1642
67290	K-T6-46	T6	0.15 mgC	95	-25	0.8972	0.0053	-102.8	5.3	870	50	AD 1041-1267
67285	K-T6-12	T6E		~99	-25	0.8401	0.0042	-159.9	4.2	1400	40	AD 592-703
67289	K-T14-45	Proxy to T6		102	-25	0.9675	0.0043	-32.5	4.3	270	40	AD 1489-1955
67288	K-T14-44	PROXY TO T6		105	-24.3	0.9038	0.0043	-96.2	4.3	810	40	AD 1170-1285
67696	K-T13-32	East Saros, East wall		150	-25	0.9698	0.0048	-30.2	4.8	250	50	AD 1489-1955
67694	K-T13-29*	East Saros, East wall	0.12 mgC	base 160	-25	0.9232	0.0065	-76.8	6.5	640	60	AD 1282-1414
67698	K-T13-35	East Saros, east wall		top 180	-25	0.8855	0.0033	-114.5	3.3	980	40	AD 999-1164
68212	K-T13-41	East Saros, east wall	shell	180	0	0.8711	0.0043	-128.9	4.3	1110	40	AD 874-1016
67697	K-T13-34	East Saros, East wall		190	-25	0.9467	0.0048	-53.3	4.8	440	50	AD 1408-1631
67286	K-T6-43	T6W @M9		200	-25	0.9777	0.0053	-22.3	5.3	180	50	AD 1655-1955
67284	K-T6-3	T6E		200	-25	0.9682	0.0042	-31.8	4.2	260	40	AD 1513-1955
67292	K-T6-43	T6W @ m9	0.04 mgC	200	-25	0.9931	0.016	-6.9	16	60	130	AD 1529-1955
67695	K-T13-30	East Saros, West wall		210	-25	0.9662	0.0048	-33.8	4.8	280	40	AD 1488-1955
67293	K-T6-6	T6E		310	-27.6	0.7638	0.0034	-236.2	3.4	2160	40	360-60 BC
67287	K-T6-6	T6E		310	-25	0.771	0.0034	-229	3.4	2090	40	190-2 BC
(dated at the Arizona AMS facility)												
Ottoman Canal Berm												
AA33511	Berm 14C-3	Tepataria Berm Trench			-25.6	0.9193	0.0055			675	50	AD 1274-1402
AA33512	Berm 14C-7	Tepataria Berm Trench			-25.2	0.7815	0.0053			1980	55	112BC - AD 191
AA33513	Berm 14C-8	Tepataria Berm Trench			-24.7	0.7976	0.005			1815	50	AD 85-371
AA33640	Berm 14C-5	Tepataria Berm Trench			-25.7	0.7985	0.0047			1805	45	AD 120-373
Kosekoy Trench 1												
68683	T1-19	above E2		3b	-25	0.9809	0.0043	-19.1	4.3	150	40	AD 1670-1955
68684	T1-6	below E2		4	-25	0.9526	0.0043	-47.4	4.3	390	40	AD 1441-1634
68686	T1-27			5c	-25	0.976	0.0047	-24	4.7	200	40	AD 1647-1955
68685	T1-25			7	-25	0.9922	0.0048	-7.8	4.8	60	40	AD 1688-1927
68687	T1-23			10	-25	0.8183	0.004	-181.7	4	1610	40	AD 381-555
68688	T1-16			11	-25	0.8281	0.004	-171.9	4	1520	40	AD 444-630

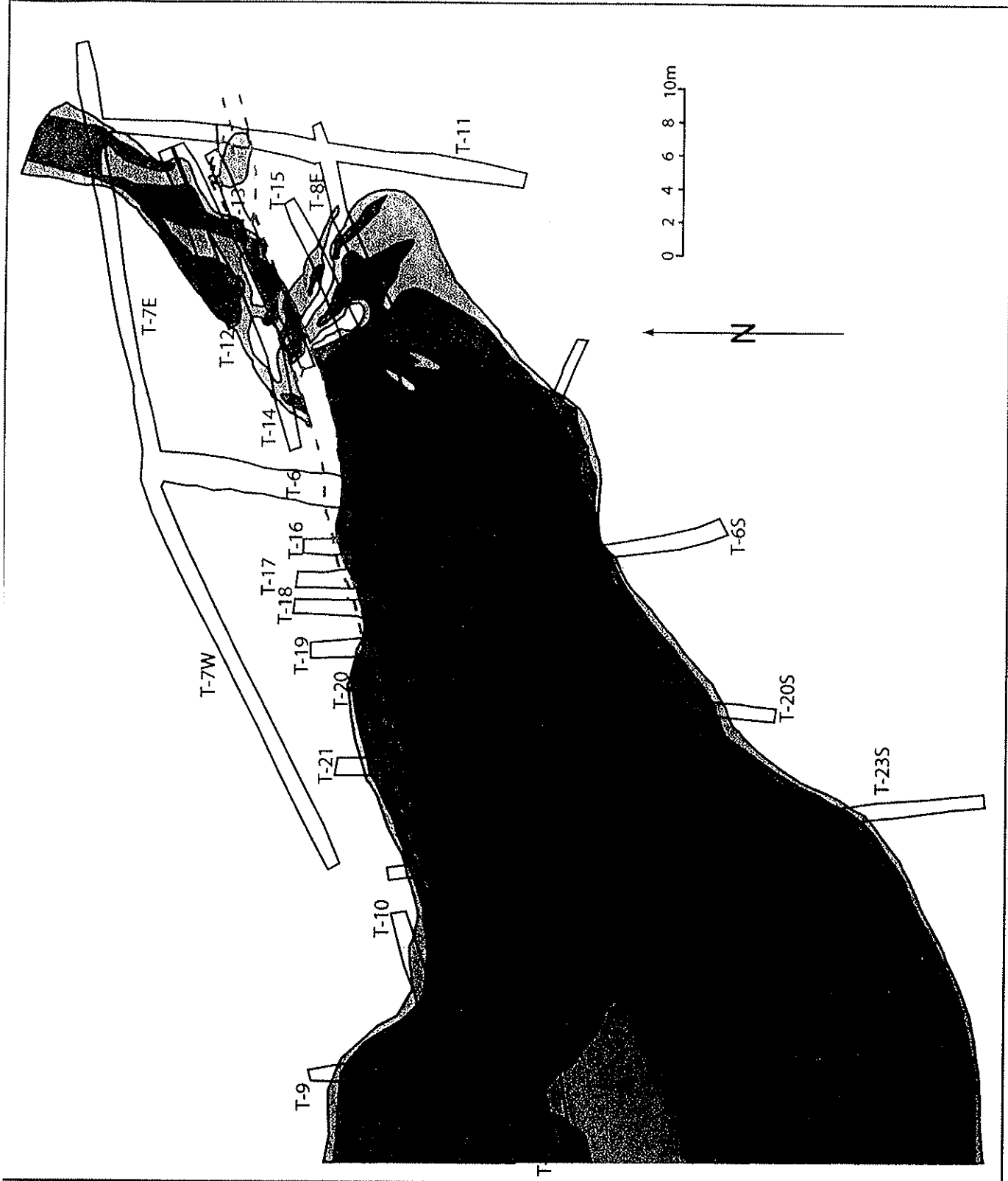


Figure 8. Isopach map of the unit 200 sand, based on nearly 1500 measurements. Note the current location of the feeder channel relative to the fan apex.

1655 and may be considerably younger. Thus, we interpret all of the C-14 samples that lie above this unit and that have older apparent ages to be the result of either reworking of detrital charcoal, or more likely, the consequence of the charcoal (and its original wood) having been resident in the system for some period of time. The post-1655 date places strong constraints on which earthquakes may have produced surface rupture at this site and added to the observed amount of offset on unit 200, as discussed below.

The stratigraphic units above unit 200 can be designated as either sedimentation within the fault zone, possibly due to formation of a depression along the fault, or the result of overbank sedimentation by the Kavak River and its tributary channels. Units 192-198, recognized in T-6E (Figure 5) and in adjacent trenches to the west, is interpreted to be a fine-grained deposit that fills a narrow trough between the unit 200 fan and a low fault scarp. Although this may be interpreted as the result of deformation along the fault, we prefer an interpretation that invokes purely stratigraphic mechanisms to produce this deposit because there is no direct evidence for a surface rupture in this part of the section. Furthermore, the isopach map of the sand in Figure 8 clearly shows a fan that splays out and flows west, parallel to the fault, thereby producing a slight low along the fault. Thus, there is no need to require a faulting event to produce this low.

In contrast, units such as 110-140 in trench T6 fill a depression that formed immediately after a surface rupture, as indicated by faulting and fissuring up to the base of that section. In these cases, the units may be only very locally preserved along the fault, although their significance to the interpretation of the event stratigraphy may be profound.

Units 10-100 are sandy to silty sediments that bury the fault scarp and are presumably derived from flood events from the Kavak River. Unit 10 is the A horizon developed in this uppermost section and is also the active plow pan in areas that are farmed, such as to the east of the highway. We dated a number of detrital charcoal samples from units 10-190 to provide preliminary constraints on the age of the overall section. Because unit 200 was found to be younger than A.D. 1655, all higher units must be as well. The C-14 results demonstrate a variety of dates ranging between about A.D. 600 and 1630, with no particular order in the section. We interpret all of these as having had a small to large component of resident age prior to their incorporation into the sediments exposed in our trenches. From this, we interpret the entire section from unit 200 to the surface as being deposited during the past 350 years or so. As this

corresponds to the part of the C-14 calibration curve that cannot be resolved without very precise ages, we did not pursue further dating of this section.

**Evidence for Earthquakes** – There was evidence observed for two large surface ruptures in nearly every trench that we excavated across the fault. In many of these, there were two deposits of well-sorted fine sand that appear to have been ejected out of the fault zone and derived from unit 200. In trench T25, we designate the earlier of these ejecta deposits as unit 195. We also observed structural evidence for two surface ruptures, with faults and fractures extending up to a specific stratigraphic level and then being overlain by unfaulted deposits. We did not construct detailed trench logs of most exposures due to the lack of time and because our focus for many of these trenches was to map out the extent of unit 200. Nevertheless, both T6 and T25 record both of these events and are discussed herein.

Evidence from trench T6 – The fault in T6 is narrow, less than 0.5 m at the base of the trench. Within this fault zone, faulting has produced liquefaction, brittle faulting, fissures, and a narrow trough into which sediment accumulated. The interpreted event horizons for each of these phenomena are coincident and correspond to the base of unit 190 and the base of unit 150.

In T6E, fractures extend to the base of unit 190 and are overlain by well-bedded stratigraphy of units 150-190. Within the fault, the section is replaced by a massive, well-sorted fine sand that we interpret as liquefaction sand derived either from unit 200 or another sand below the base of the trench. In some trenches, we exposed a deeper well-sorted sand below unit 350, and considering that the pipe extends to the base of the trench, we interpret the lower sand as the most likely source. This liquefaction sand is also overlain by unit 190 along both margins of the fault zone in this exposure. Finally, along the northern edge of the fault zone, a narrow depression is filled by finely laminated stratigraphy of units 150-190. We interpret the depression to be a direct result of a surface rupture.

East of the highway, we constructed detailed logs of the fault zone in trench T25 to further constrain the timing and number of events that post-date the unit 200 sand. At the time of the field exercise, we did not know that the sand was younger than can be adequately addressed with C-14. Nevertheless, our observations provide additional constraints on how many events post-date unit 200. It should be noted that the earlier study by Rockwell et al. (2001) also found

evidence for only two surface ruptures after deposition of their unit 3, which is identical to unit 200 described herein. Trench T25 lies within 10 m of Rockwell et al.'s (2001) trench T-1.

In the east wall of T25, the northernmost fractures extend up through unit 200 and are overlain by another clean sand (unit 195) that we interpret as ejecta derived from unit 200. Massive clean sand fills the main fault and is also interpreted to be the result of liquefaction of unit 200. Overlying unit 195 is a sequence of bedded silt and sand units (units 160-190) that are not faulted by the northernmost strand of the zone. These observations all indicate a surface rupture that occurred when unit 200 was at the surface.

Another set of fractures displaces all units up through 160, including unit 195 (liquefaction sand from the penultimate event). Chunks of bedded stratigraphy, comprised of units 160-190, lie floating within the fault zone in a massive, fine sand matrix that we interpret as the result of re-liquefaction of the unit 200 sand.

In the west wall, similar relationships indicate two liquefaction events, one immediately after deposition of unit 200 and another after deposition of unit 170. After the second liquefaction event, finely laminated silt and sand was deposited on the southern, downthrown side of the fault. There is not clear evidence for two fracturing events, presumably because the most recent event re-liquefied material and erase such evidence. Nevertheless, the vertical separation of unit 200 is considerably more than that of unit 190, indicating more than one event. Further, unit 195 is again interpreted as liquefaction ejecta that resulted from the earlier event.

The above observations indicate two surface ruptures preserved in the stratigraphy, one at the contact at the base of unit 190 and one before deposition of unit 150. These are identical to the relationships determined in trench T6 and we interpret these to be the same two events. Thus, at these and all other exposures that we examined in our field exercise, we note evidence for two ruptures that produced liquefaction, surface faulting, and consequent sedimentation along the fault. Both of these events must have occurred after deposition of the channel sand of unit 200, or after A.D. 1655. The only two large events that may be ascribed to these surface ruptures are the large regional events of August 1766 and November 1912 (Ambraseys and Finkel, 1987a, 1987b, 1995, Rockwell et al., 2001). Thus we attribute lateral slip on unit 200 to be the cumulative result of these two earthquakes.

Determination of Lateral Slip – The channelized nature of unit 200 is ideal for resolving cumulative slip for the two events that post-date its deposition. From the aerial photographic analysis, it appeared that the paleo-channel containing unit 200 flowed at a high angle to fault. We chose the area west of the highway to conduct the detailed 3D portion of this study because the area is devoid of agriculture and we were unrestricted in our ability to excavate long trenches both across and parallel to the fault zone.

In the preliminary excavations such as trench T6, we were not certain as to the aerial distribution of the unit 200 sand, so we began fault-parallel excavations to determine its extent. In all, we excavated 19 trenches and trench extensions to resolve the geometry of the unit 200 deposit. All exposures were surveyed with a Wild TC 2000 total station to provide accuracy. Further, a surveyed string line was emplaced in all trenches at the same elevation to assure accurate measurement of the sand thickness and the relative elevations of its top and base. Because we couldn't make detailed logs of all exposures in the amount of time we had in the field, we instead took over 1500 detailed measurements on the thickness of the sand, including the exact locations of the pinch outs, to construct an isopach map of its distribution (Figure 8).

Unit 200 is much thicker on the south side of the fault than on the north. We take this to indicate that a low scarp was present at the time the channel flow across the fault. North of the fault, the sand is confined to a narrow channel and never exceeds 20 cm in thickness. The channel slopes to the south, towards the fault, and then thickens to over 40 cm where it crosses the fault. The overall form is that of an alluvial fan, and we interpret the channel to have splayed across the fault scarp, resulting in deposition of the main fan on the south side. The fan deflects downstream, towards the coast to the west, and only extends south of the fault for 5-10 m. As seen in trench T6, the fan has a convex-up cross profile and is multi-lobed. The apex of the fan is exposed in trench T15, and the fan rapidly thins to the east and pinches out in trenches T8 and T15. To the west, the fan is bound on the north by the fault for a distance of about 30-35 m, and then the edge of the fan crosses the fault with 10-15 cm of deposition north of the fault. In the vicinity of T6 and the area of the feeder channel, unit 200 is thickest away from the fault except at the fan apex.

We reconstruct the fan apex with the deepest portion of the feeder channel to resolve about 9 m of lateral slip (Figure 9). A secondary smaller channel west of the main channel also reconstructs to a secondary fan apex, and the margins of the fan to the east of the feeder channel

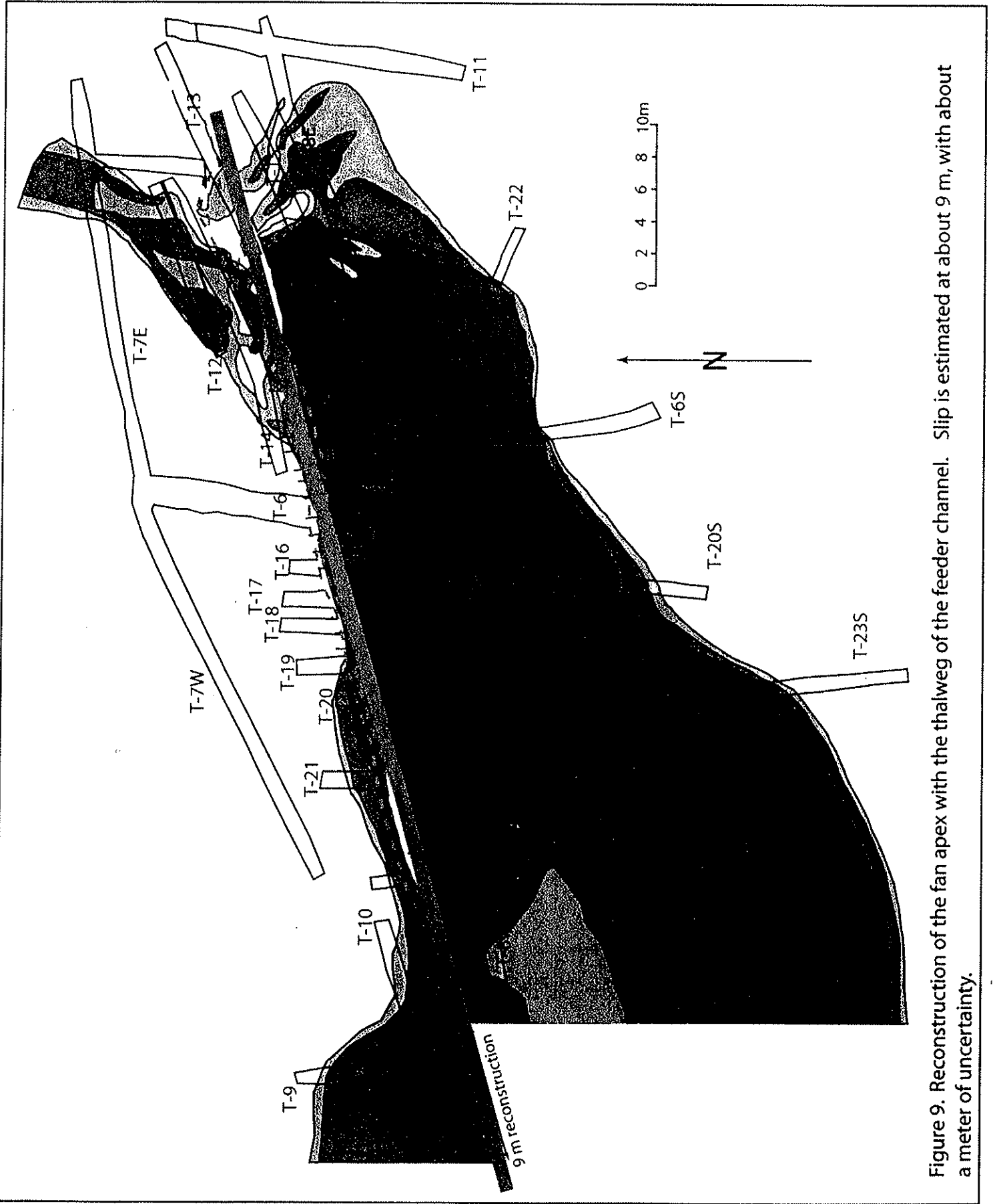


Figure 9. Reconstruction of the fan apex with the thalweg of the feeder channel. Slip is estimated at about 9 m, with about a meter of uncertainty.

all realign. Furthermore, the thickest portion of the fan that ponded adjacent to the fault west of T-6 realigns to the thinner section of sand that spilled across the fault to the north. The uncertainty in the 9 m estimate is on the order of about a meter, based on the realignments and their mismatches if the reconstruction is less than 8 m or greater than 10 m. We take this  $9 \pm 1$  m value as the cumulative slip produced by both the 1766 and 1912 earthquakes. If each earthquake produced similar slip at this site, then the ~4-5 m of presumed slip is similar to the average values for many of the large earthquakes that have ruptured the North Anatolia fault this century. It is also consistent with the amount of slip predicted by Ambraseys and Finkel (1987) for the 1912 earthquake, based on the inferred size and expected amount of slip.

### **Izmit to Sapanca Segment**

We initiated paleoseismic studies along the Izmit-Sapanca fault segment in October 1998 prior to the earthquake. In our preliminary work, we focused on dating a canal feature that was possibly the result of an effort by the Ottomans in 1591. After the earthquake, we returned to the canal to resolve how many earthquakes had affected the canal stratigraphy. We also began trenching west of the end of the canal along a small fluvial channel in the township of Kosekoy with the purpose of resolving a longer record. As will be shown, the records at both sites are similar and only record fault activity for the past 400 years or so.

The Ottoman Canal Site –Multiple periods of canal construction have been discussed in the literature (Finkel and Barka, 1999), with at least two known efforts of excavation. The earliest effort is pre-Roman and was intended to connect Lake Sapanca with Izmit Bay, thereby opening up commerce and access to the inland forests and other resources. A number of subsequent efforts were “discussed” (mentioned in court records, etc.) although most of these were never undertaken. The most recent effort, for which there is direct historical documentation and known expenditures, was undertaken by the Ottomans in 1591. In a preliminary effort in 1998, we excavated the south margin of a large, abandoned canal at Tepetarla with the purpose of dating the construction of this prominent feature that crosses the fault zone between Tepetarla and Kosekoy. The canal extends from near Lake Sapanca westward about half of the distance to Izmit Bay, consistent with historical accounts for the 1591 effort. The purpose of our initial trench was to resolve whether this was the Ottoman effort of 1591 or an earlier canal effort.

We observed that there were numerous pieces of small to large detrital charcoal, some that were associated with burn zones, that we interpret represent cooking fires or fires to boil water for tea (as is a common practice today in Turkey). We collected eight large samples and dated four of the samples to place maximum ages on the berm construction, and therefore the canal excavation project. In that it is likely that the workers burned dead wood for their fires, and as there are numerous large trees in the area today, we surmise that all of the samples will be older than the actual age of the berm. As it turns out, the ages of the detrital charcoal pieces range from a maximum age of 112 BC to as young as AD 1402 (Table 1). We therefore infer the berm and canal construction to post-date the youngest sample dating to the 14<sup>th</sup> century, and to be the effort funded by the Ottomans in 1591. Thus, all of the alluvial fill within the canal must date to younger than 1591 so we did not attempt further C-14 dating in the canal fill.

In the summer of 2000, we excavated a trench across the 1999 rupture west of Tepatarla where the fault is entirely contained within the canal fill (Figure 1). The trench site was chosen about 2 meters west of a small several-meter-long open extensional fissure resulting from a 1 meter-wide releasing step-over. The trench exposed predominantly fine-grained, bedded clayey canal fill, although a distinctive sand was found to fill a fissure zone within the fault zone, apparently resulting from a prior rupture (Figure 10). The fault zone is approximately 3 meters wide in the trench, although the 1999 rupture zone is narrower.

The stratigraphy was differentiated into nine units, with the topmost and youngest unit (unit 1) interpreted as a plow pan. Unit 1 is a massive silty clay, similar in texture to several of the underlying strata. Unit 2, which is bedded and further subdivided into several subunits, is in part an alluvial fill within the fault zone. Unit 2a is a fine silty sand that is only present north of the 1999 rupture trace. Unit 2b is clayey silt that fills a depression within the fault zone. In contrast, unit 2c is a coarse gravelly sand which not only fills the depression in the fault, but also extends downward in the fractures to the base of the trench. This unit grades upward in to sand at its top. Unit 2d is well-sorted fine sand and we interpret this unit to be the result of liquefaction and is likely derived from a clean sand below the base of the trench. Units 2a through 2d may comprise a fill sequence in a fissure within the fault zone following an earthquake.

Unit 3 appears to be a buried topsoil unit that was incorporated into the fault zone and bound by fault strands from an earlier event. Unit 4 is a massive pebbly clay to clayey sandy silt (varies laterally) that grades down to the pebbly silty clay strata of units 5 and 6. These units are

# Ottoman Canal Site

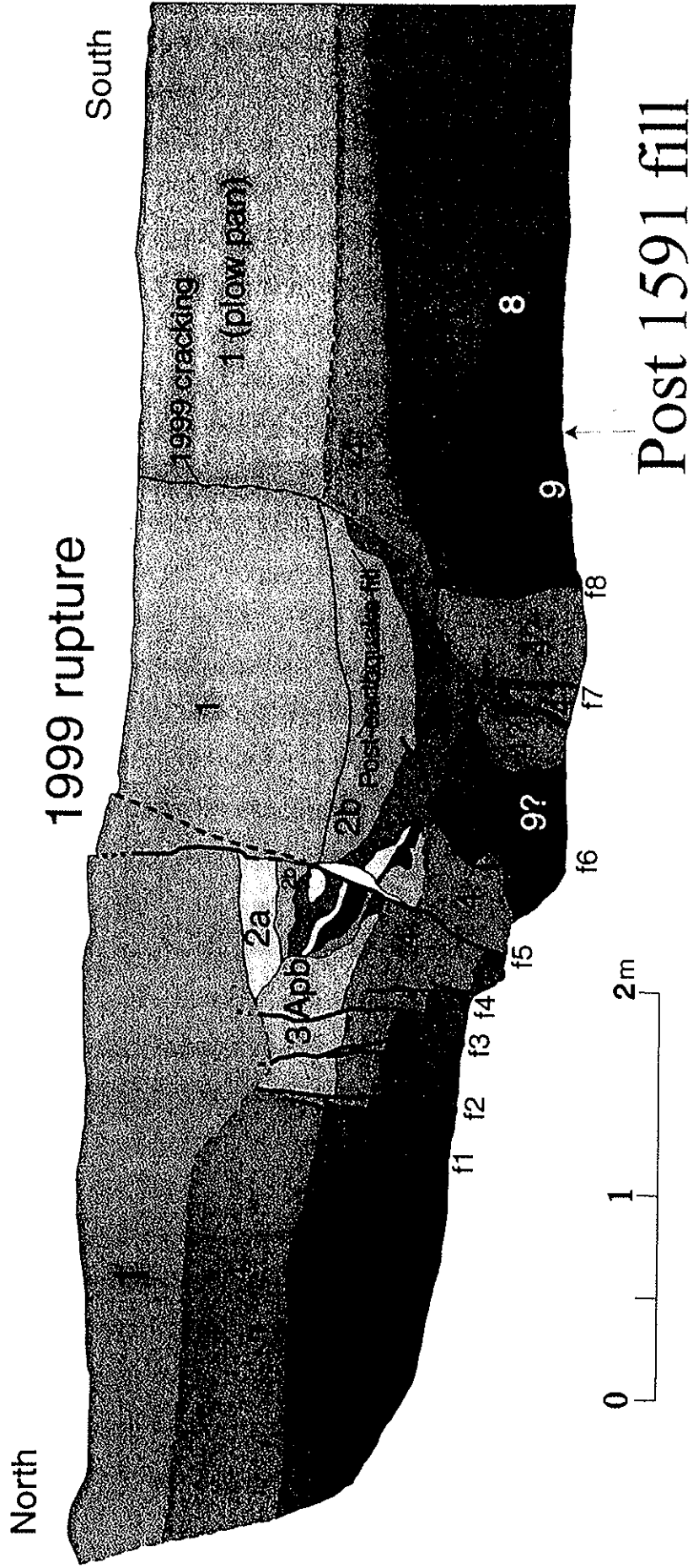


Figure 10. Trench log of the Ottoman canal site near Tepatarla. The 1999 rupture produced slip in a narrow zone, with minor cracking over a 2 meter width. All deposits exposed in the trench post-date the excavation age of the canal, 1591.

interpreted as quite water canal fill alluvium, although the presence of scattered pebble clasts may alternatively suggest a debris flow origin. Unit 7 is an oxidized, finely bedded silt grading downward to sand, whereas unit 8 is a well-sorted sand. Unit 9 is a sandy gravel of probable fluvial origin, and units 9 through 7 apparently represent a fining upward fluvial sequence. The unit designated as 9? Within the fault zone is lithologically similar to both unit 9 and unit 2c and may be part of the section that liquefied or was mobilized during liquefaction of unit 9.

We did not directly radiocarbon date any of the strata within this trench, although detrital charcoal was abundant and we collected over 50 samples from this trench. However, as the base of the canal was not encountered (the base should be greater than 5 m depth), we infer the entire section to post-date A.D. 1591. In that many or most samples likely have some residence age (growth plus burning prior to burial), and because of problems with calibrating C-14 dates after about A.D. 1600, we did not see the utility in spending the effort to further date the section. Nevertheless, all earthquakes recorded at this site must also post-date A.D. 1591, which is fairly well-recorded in the history for this region.

Evidence for Prior Earthquakes – There is clear structural and stratigraphic evidence for at least one and possibly two events prior to that of 1999. For discussion purposes, we have numbered the individual fault cracks as f1 through f8 from north to south. In a couple of cases, minor faults are grouped with more major ones. Several of these faults moved in at least one prior event, whereas only a couple appear to have been reactivated in 1999, which is referred to as event E1.

The 1999 (E1) rupture localized along a narrow crack, fault f5, near the center of the trench and displaces all strata up through unit 1 to the surface. A second surface crack aligns with fault f8, and this fault becomes the edge of a 2-m-wide pull apart that produced a narrow sag in 1999 only 2 meters east of this trench face. In the trench wall, this fault appears to have only cracked and no evidence of any significant displacement could be resolved. The base of the soil may be offset by a couple of centimeters, but that was not clear. Below the cracked soil, however, fault f8 defines the southern edge of the fault zone and was clearly active and a main player in an earlier event. Along fault f5, the principal 1999 displacement surface, different units are juxtaposed and similar units have significant variations in thickness across the fault. We attribute these relationships to the ~3-4 m of lateral slip recorded for the 1999 earthquake in this vicinity.

At least one earlier event, E3, is strongly indicated by the occurrence of a number of fault strands that break units 3-9 but are overlain by the unbroken soil of unit 1. Fault f2 drops an older topsoil horizon, unit 3, down against units 4 and 5, and the mismatch in unit thicknesses across this fault indicates substantial lateral slip. Faults f1, f3 and f4 also cut units 3 through 7 but are overlain by unit 1. There is no indication that any these faults were activated in 1999. Faults f6, f7 and f8 also appear to have activated in this earlier event, which apparently resulted in an open fissure at the surface that was subsequently filled by unit 2. Unit 2d is a fine sand that may be the result of a sand blow. Unit 2c, in contrast, is a gravelly sand that is intrusive downward into the fault zone and is very similar to the sandy gravel of unit 9. We observed gravelly sand mobilized during the 1999 earthquake, resulting from liquefaction and lateral spreading on the shoreline at Sapanca, so we surmise that this gravel may also be a consequence of liquefaction, in spite of its coarse nature. In any case, the occurrence of the unit 2 deposits precisely within the fault zone virtually requires that an open fissure was present after deposition of unit 4 and the development of the soil of unit 3. We attribute the presence of the unit 2 deposits to this earlier faulting event.

A third event that is intermediate in age between events E1 and E3 is suggested by the breakage of the unit 2 fill by fault f6, which juxtaposes units 2d and 4, and causes a significant mismatch in the thickness of unit 2c. The upward termination of fault f6 appears to be in unit 2b, and we could not trace any evidence of this fracture upward to the modern ground surface. Based on the mismatch in stratigraphic thicknesses and the juxtaposition of dissimilar units, we infer that this fault must have significant lateral slip. The problem with a surface rupture interpretation at this stratigraphic level is that unit 2b apparently fills the depression left by event E3 and it is difficult to believe that the depression lasted for too long after the surface rupture. Thus, event E2 must have either occurred soon after event E3 or the site was closed to significant deposition for some extended period of time after event E3, which is possible considering the sites presence within the canal.

An alternative explanation is that fault f6 deformation is absorbed in the fine-grained fill of units 2b and 1 and that this fault was activated in 1999. Support for this idea is weak, but is based on the inference that unit 2b is only slightly younger in age than unit 2c, which appears to have directly resulted from the earlier event. However, the evidence for lateral slip along fault f6 is strong and would require a significant amount of strain being absorbed in unit 2b.

A third possibility is that unit 2c is a fluvial deposit that filled/eroded along the fault after event E3 and was faulted by both faults f6 and f7 during event E2. The fissuring of unit 2c downward into the fault could be explained by this mechanism and therefore would not require liquefaction of the sandy gravel of unit 2c.

We attribute event E3 to the large event of 1719 that had descriptions of damage that closely parallel those of 1999. It is the first large event after 1591 for this area and was apparently as large as 1999, consistent with the trench observations that indicate event E3 was a major surface rupture. Considering the case that event E2 occurred soon after that of E3, we attribute that deformation to either afterslip or possibly the 1754 earthquake, which is known to have produced damage in this region but for which the source is unknown. Later earthquakes, such as 1878 or 1894, appear to have occurred too long after event E3 and the surface soil of unit 1 would almost certainly have developed by that time.

The Kosekoy Site – The Kosekoy site lies along a section of rupture in the southeast corner of the township of Kosekoy, south of Izmit and west of the end of the Ottoman canal. Rupture in this area in 1999 included about 2 m of slip along the primary fault strand, and secondary rupture along faults that splay off to the north from the main strand. Rockwell et al. (2002) report offsets of surveyed trees adjacent to this site to be on the order of 1.8-2.25 m, consistent with slip values reported from rupture mapping after the earthquake (Barka et al., 2000). To both the east and west of the Kosekoy area, slip along the Izmit-Sapanca rupture segment generally exceeded 3 m in 1999, and slip values as high as 3.8 m based on surveyed data were reported by Rockwell et al. (2002). We interpret this to mean that slip is distributed across multiple strands in the Kosekoy area. We chose this site in part because the secondary faulting could be demonstrated to be principally dip slip, making past earthquake recognition and reconstructions easier. Furthermore, paleo-earthquake events can often be easier to recognized where multiple fault splays are present as some secondary faults may rupture in only one or two events. Finally, part of our group (Ferry and Meghrouri) conducted radar profiles at this site and identified an offset buried paleo-channel that is apparently offset about 6.6 m, roughly three times the 1999 slip. We had also hoped to establish a longer record than that at the Ottoman canal site, but as will be shown, the upper 2 m of section generally covers the same time period – the past 400 years.

We excavated five trenches at this site (Figure 11), with only trench 3 crossing the main fault. Trench 1, which is presented in detail (Figure 12), was excavated across a purely dip-slip fault that experienced about 60 cm of slip in 1999. A nearby small flume displayed no evidence of lateral slip (Figure 11), thereby confirming the normal slip inference for the fault in trench 1. Thus, no out-of-plane transfer of sediments is expected and past events should be recognized by similar dip-separations.

The stratigraphy in trenches T-1 and T-3 is composed of a sequence of coarse and fine-grained strata that are interpreted as fluvial channel and overbank deposits (Figure 12). Unit 1 is a dark brown plow pan (topsoil A horizon) unit that was tilled frequently. Units 2 and 3 are bedded channel deposits, with unit 2 being a distinctive sandy gravel and unit 3 being a stratified coarse to fine sand. These units pinch out to the north across a paleo-scarp (Figures 12) and locally scour into the underlying unit 4. We interpret this part of the section to represent a period of sedimentation prior to the current incision of a drainage located a few meters south of the southern end of trench T-3.

Unit 4 is a dark brown, massive, clayey silty sand (loam) that we interpret as a buried A horizon or topsoil. This unit was easily mappable south of the fault but north of it, unit 4 appeared to become less distinct so we grouped it with unit 5 to the north. Unit 5 itself is a weakly stratified clayey silt with sand that grades downward to a pebbly, sandy clayey silt. North of the fault, the equivalent unit, unit 4-5 is a massive pebbly clayey silt that we interpret as a colluvial unit.

Unit 6 is a very distinctive plastic clay that was only exposed south of the fault and appears to thicken towards the fault. We interpret unit 6 as an overbank deposit, although it may be clay derived from overbank sedimentation ponded within the fault zone. Unit 7, in contrast, is a gravelly clayey silt that appears very similar to unit 5. The gravel content is sparse away from the fault but increases towards the fault, suggesting a colluvial origin for this unit as well. Finally, south of the fault, unit 8 is a distinctive coarse sand interpreted to be fluvial in origin. This sand was traced laterally towards trench T-3 and forms the channel deposit imaged by Ferry and Meghrouri in their radar survey.

North of the fault, trench T-1 exposed several older units below unit 4-5. Unit 9 is a bedded coarse sandy, clayey gravel interpreted to be fluvial in origin. There was no equivalent for this unit exposed south of the fault, although it is the probably source for the gravelly

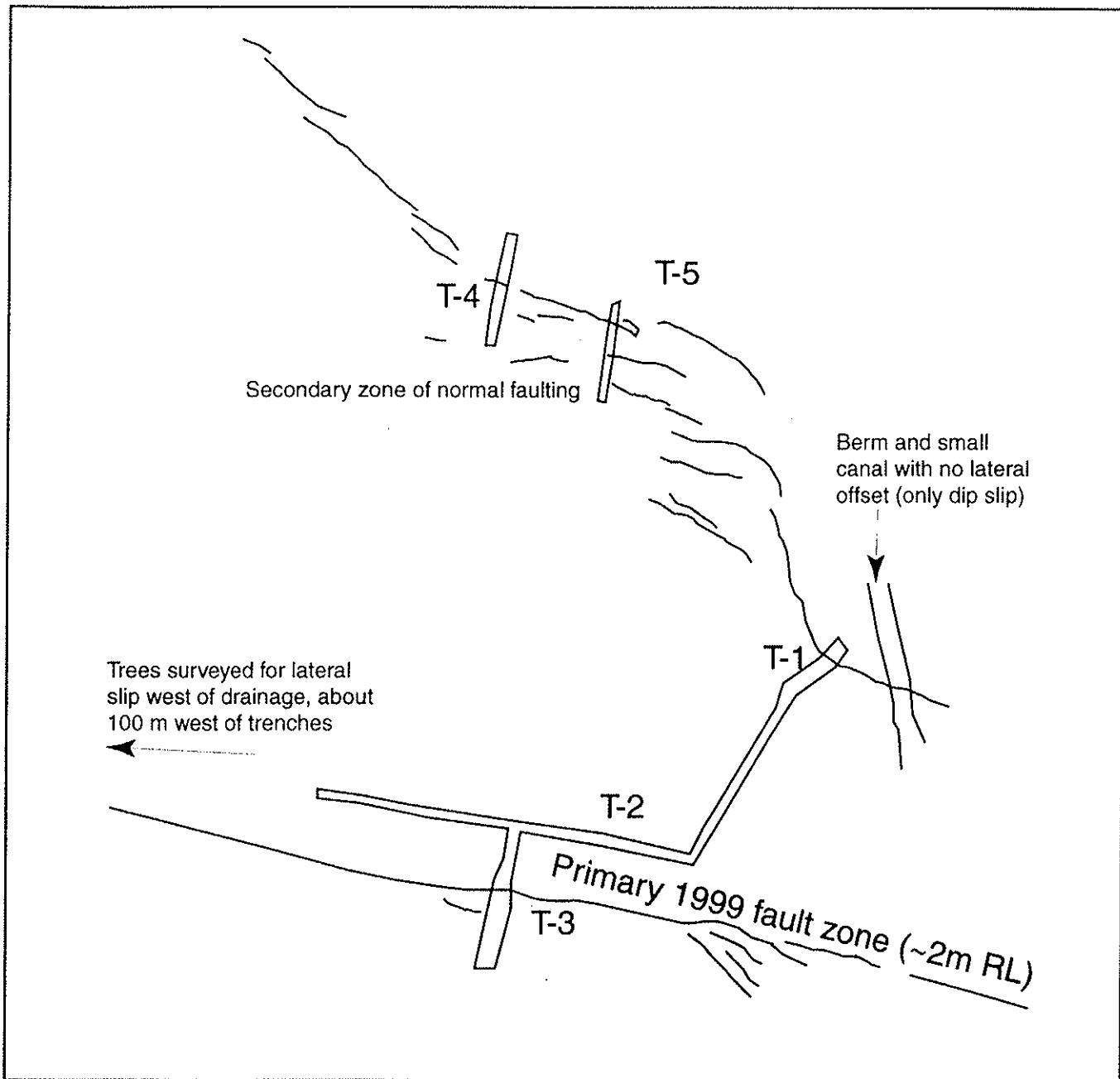


Figure 11. Map of trenches at the Kosekoy site. About 2-2.2 m of right-lateral slip was noted for the main fault after the 1999 earthquake. The secondary zone of faulting experienced primarily normal (extensional) faulting at this site, and may connect to a second strike-slip zone to the west. Rockwell et al. (2002) report between 1.8 and 2.25 m of slip at their site 11, located about 100 m west of our trenches. They also report higher values of 3-3.5 m both east and west of the Kosekoy area, indicating that significant off-fault deformation may be representative for this stretch of the 1999 rupture.

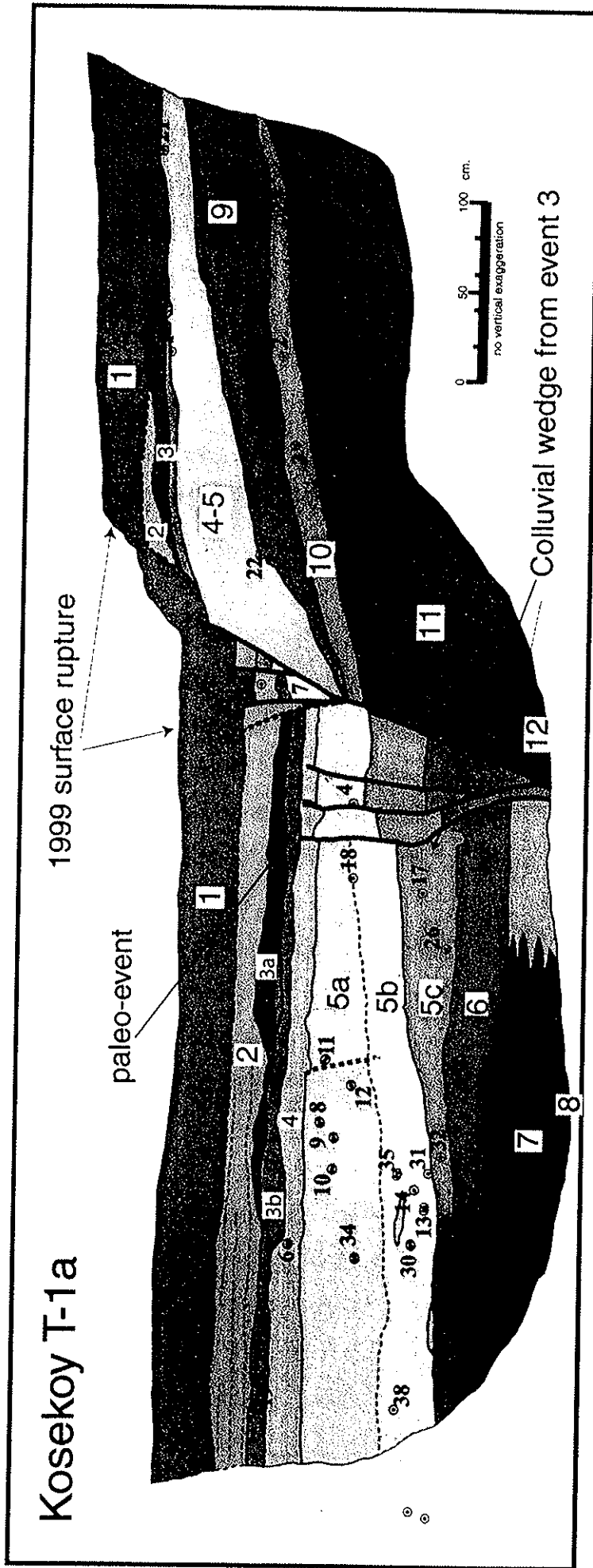


Figure 12. Log of the Kosekoy trench T-1. Slip in 1999 was purely dip-slip, based on the lack of lateral offset of an adjacent flume. Note the older fractures that did not rupture in 1999. Red dots with numbers are detrital charcoal sample locations. Larger numbers in white boxes are unit designations. All unit descriptions are in the text.

colluvium of unit 7. Unit 10 is a distinctive silty fine sand with scattered gravel, unit 11 is a coarsely bedded gravel containing abundant pottery and tile shards, and unit 12 is a distinctive coarse sand. Collectively, units 9 through 12 are interpreted as a fluvial sequence of strata preserved on the northern upthrown side of the fault zone.

Age control for the stratigraphy in T-1 is provided by dating of individual detrital charcoal samples. Charcoal was abundant in our exposures, and we collected over 200 samples from the Kosekoy site. In T-1 alone, nearly forty samples were collected and we dated six. Four samples were dated from units 3 through 7 and two from the older units north of the fault.

All four samples from units 4-7 yielded modern or nearly modern results. The sample from unit 7 yielded a calibrated age of AD 1688-1927, requiring that all overlying units are also no older than 1688. Thus, most of the exposed section south of the fault was deposited during the past 335 years or so.

North of the fault, two samples were dated from units 10 and 11, with the lower sample from unit 11 yielding a slightly younger calibrated date range of AD 444-630. As both sample ages are indistinguishable at 2s, and as they both place the age of these units at about the 5<sup>th</sup>-6<sup>th</sup> century AD, we accept these dates as the approximate age of this older fluvial section. Thus, there is over a thousand year hiatus in deposition on the northern side of the fault, although much of the record may be preserved at depth below the current base of T-1 to the south.

Interpretation of Past Earthquakes – We recognize evidence for at least one and possibly two events recorded in the stratigraphy south of the fault exposed in T-1. The most recent event is obviously the August 1999 Izmit earthquake, and is designated as event E1. Earlier events are easiest to recognize once the 1999 deformation is removed. In that the 1999 earthquake produced no lateral slip at trench T-1, we reconstruct the pre-1999 section assuming no out-of-plane motion (Figure 13a), which required about 53 cm of dip reconstruction.

Evidence for the penultimate event (prior to 1999) is clear in Figures 12 and 13, where several secondary strands break up through unit 4 but are planed off and buried by unit 3. Unit 3 also pinches out north of the fault, indicating the presence of a scarp at that time. In the reconstructions of Figure 13a, these relationships are even more obvious, with units 2 and 3 pinching across a buried fault scarp produced by the penultimate event. Units 6 through 4 are faulted by the secondary strands and overlain by units 1-3. A degraded scarp supported by units

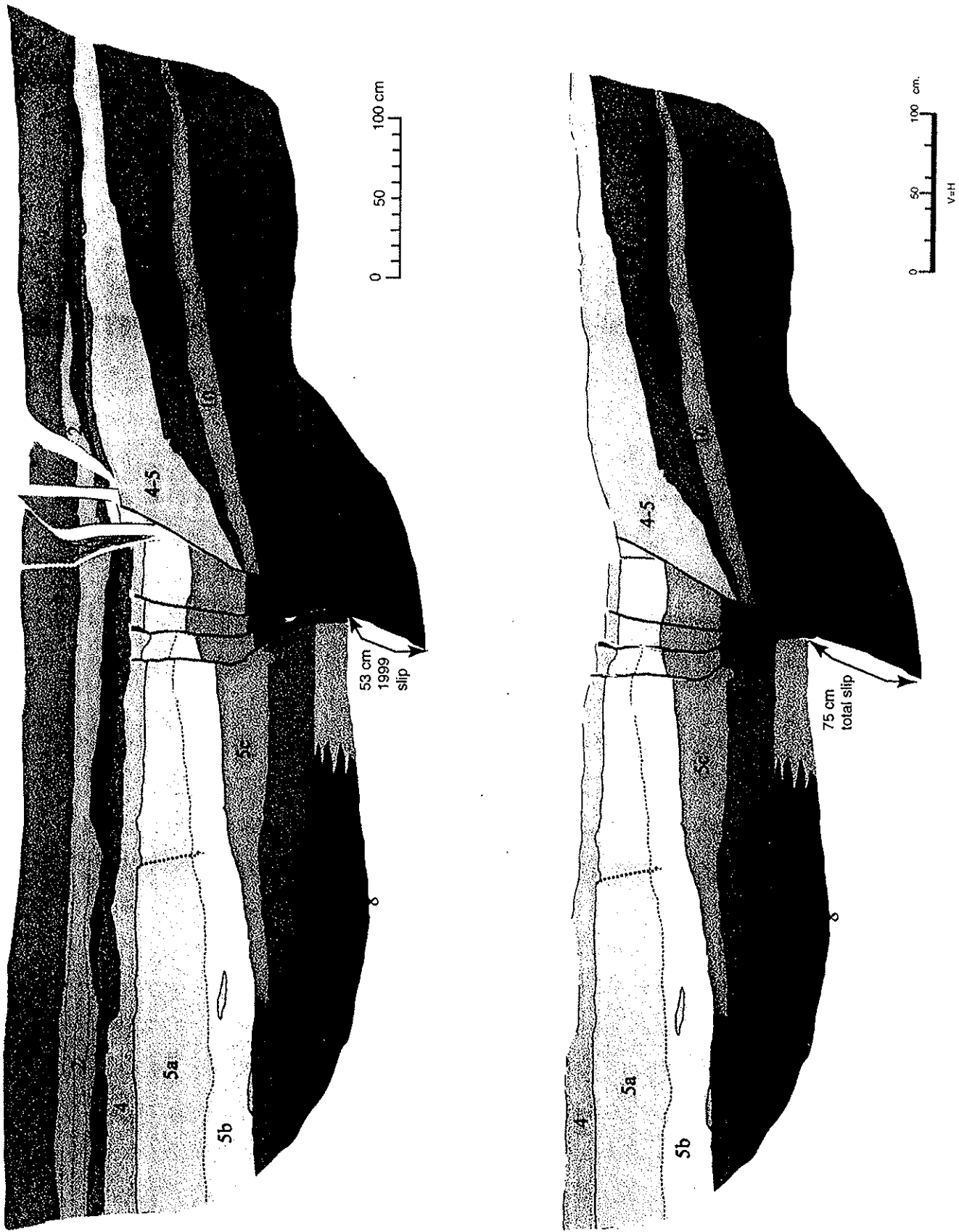


Figure 13. Reconstructions of the log from trench T-1 at Kosekoy. In the upper diagram, the effects of the 1999 earthquake are removed, and the original ground surface restored to near horizontal - its original configuration. In the lower reconstruction, the effects of the penultimate event have been removed, assuming purely dip-slip displacement.

4 and 5 is evident. From these observations, we interpret event E2 to have occurred after the deposition of unit 4 and prior to the deposition of unit 3. Based on the ages of these units, E2 must have occurred after AD 1688.

We attempted to remove the deformation of event E2 with further reconstruction of the units faulted in E2 (Figure 13b). We reconstructed units 4-6 across the secondary strands, and restored or re-matched units 4 and 5 south of the fault to unit 4-5 north of it. This required an additional 22 cm of reconstruction, or about half of that required to remove the 1999 deformation. This reconstruction resulted in an apparent depression along the fault, part of which is explained by the subsequent uplift and erosion of unit 4 during and after event E2. The balance is explained by erosion of unit 4-5 on the north after the formation of the scarp. The volume represented by this depression was evidently removed by the unit 3 channel deposits.

Several important observations can be made about an earlier event, E3, from the reconstruction presented in figure 13b. First, units 4 and 5 appear to have been deposited against and across a scarp underlain by unit 9 north of the fault. This interpretation is based on the observation that these units pinch out northward, similar to what happened to units 2 and 3, requiring the presence of such a scarp. However, in detail, unit 5c is thickest at the fault and thins southward, indicating that it may be a colluvial wedge derived from the scarp itself. This would require that the lower part of unit 4-5 was already present at the time of the event. In this case, unit 4-5 is older than unit 5 and our numbering scheme is in error. Alternatively, units 4 and 5 (and 4-5) represent slow accumulation of colluvial materials across a scarp, largely derived from uphill to the north, and the wedge-like appearance of unit 5c is in part due to the massive character of unit 4-5 north of the fault and non-recognition of that contact. In this interpretation, event E3 occurred before deposition of unit 5 altogether.

In the reconstruction in Figure 13b, units 6 and 7 appear to be in fault contact. This requires that they were either faulted down into this position or that they were deposited against the scarp (or derived from it) after an event. In that the relationships within the fault zone have been obscured by the two subsequent events, either interpretation is permissible. Unit 6 is very fine-grained clay that is only present south of the fault and thins to the south. The thinning may be an artifact of our limited exposure. Nevertheless, it is thickest at the fault. This may be localized quiet-water sediment within the fault zone due to the presence of a depression. This would require an event after deposition of unit 7, and there is no other evidence for this assertion.

Unit 7, in contrast, has the appearance of being a fault-derived colluvial unit, as it is coarsest at the fault and fines southward. This observation suggests that it was derived off of a scarp to the north, possibly in large part to erosion of units 9-11. If this is the case, then event E3 occurred shortly before deposition of unit 7.

The above observations are not all consistent on when event E3 occurred. Nevertheless, it is difficult to envision how units 4 through 7 were deposited in the current configuration without a scarp-forming event, as that would have required a steeply dipping free face exactly coincident with the fault.

Another observation that is consistent with the occurrence of three events after deposition of unit 8 is based on a radar survey conducted by M. Ferry and M. Meghrouri at this site (Ferry and Meghrouri, personal communication). Prior to our trenching, they ran radar surveys parallel to the 1999 rupture and imaged a buried channel on each side of the fault. North of the main rupture, we encountered this channel in our trench 2. The channel deposits fine northward to become the coarse sand of unit 8. South of the fault, the interpreted correlative channel is lateral displaced about 6.5 m westward. We attempted to trench to the depth of the channel. However, saturated conditions and a collapsing trench wall precluded a direct look at this deposit south of the fault. If the radar correlation and estimate of slip is valid, approximately three times the amount of slip as occurred on the main rupture would be required to restore the lateral offset of the unit 8 channel. This is consistent with our inference that three events are required to explain all of the relationships observed in trench T-1.

Event E1 is the 1999 Izmit rupture. Event E2 is possibly the large 1719 earthquake that apparently broke the same section of fault based on historical accounts (Ambraseys and Finkel, 1995). However, our observations suggest the vertical slip in event E2 was smaller than that of 1999 whereas the 1719 earthquake appears to have been as large. It is possible that 1719 ruptured through the site from a different direction, making displacement observations on secondary faults of less value. It is also possible that this secondary fault displays variable amounts of slip in each earthquake. Another possibility is that event E2 is more recent than 1719, and is possibly 1754.

Event 3 must have occurred after deposition of unit 8 but before unit 5. The detrital charcoal date on unit 7 indicates that it is no older than AD 1688. Thus, it is possible and even

likely that both events E2 and E3 post-date 1688. If this is the case, then event E3 may be the 1719 surface rupture.

### **Discussion of Results**

We have demonstrated that west of the Marmara Sea step-over along the Saros-Ganos fault, ~8.5 m of lateral slip has been released along the North Anatolia fault during the past few hundred year. We have identified two large surface ruptures that produced this slip, and the historical record indicates that these are probably the large regional earthquakes of August 1766 and November 1912.

To the east of the Marmara Sea, we excavated trenches across the 1999 Izmit rupture at Kosekoy and in a 1591 Ottoman trench. At both sites, we can demonstrate that three surface ruptures have occurred at each site. In the case of the Ottoman canal, we can only constrain these to post 1591. At the Kosekoy site, however, it appears that all three post-date 1688. Furthermore, the middle event, E2 at each site, appears to be the smallest of the three. These may be the earthquakes of 1719 and 1754, with the latter being arguably smaller based on historical accounts (Ambraseys and Finkel, 1995). Slip in these three events is inferred by a radar survey (Ferry and Meghrouri, personal communication) to be roughly three times that which occurred in 1999. The 1999 main rupture trace at Kosekoy had low slip relative to sites to the east and west (Rockwell et al., 2002), probably related to some off-fault deformation. If the  $3\pm 0.5$  meters of slip is more representative for the Izmit segment, as implied by Rockwell et al. (2002), then as much as 9-10 m of slip may have occurred along the Izmit segment in the past 330-410 years. Thus our results indicate similar amounts of strain release during the past several hundred years both to the east and west of the Marmara Sea.

Hazard to Istanbul - An assessment of the likelihood of a large earthquake beneath the Marmara Sea near Istanbul must account for not only the recent behavior of the North Anatolian fault, as has been done by Parsons et al. (2000), but the past history of the fault zone based on paleoseismology.

The North Anatolian fault has experienced a sequence of earthquakes this past century that is unprecedented. The fault zone has essentially unzipped from east to west in this sequence, beginning in 1939 with the M7.7 Erzincan earthquake. A westward progression of earthquakes

followed, with large ( $m > 7$ ) earthquakes rupturing westward in 1942, 1943, 1944, 1957, 1967 and 1999 (Stein et al., 1997) (Figure 1). There were also earthquakes that occurred to the east after the 1939 event. The 1999 earthquakes culminated this sequence, with  $\geq 4$  m of rupture now having occurred along the entire fault since 1939 from east of Erzincan to about the Hersek peninsula, west of Gulcuk.

West of the Marmara Sea, the North Anatolian fault experienced rupture in the 1912 earthquake from the Marmara to at least the Gulf of Saros, which followed an M7 earthquake to the west in 1893 offshore in the Gulf along the Greek coast line (Nick Ambraseys, personal communication). Thus, the NAF has experienced rupture along most of its length this century, except in the vicinity of the Marmara Sea.

Stein et al. (1997) used a model of increasing Coulomb stress to explain the westward progression of failure. They predicted that the Izmit section, west of the 1967 surface rupture, was likely to go next and gave a high probability of failure during the subsequent 30 years. Their prediction was followed by the Izmit and Duzce earthquakes only two years later in 1999. The Duzce earthquake filled in a gap along a northern strand; the 1967 Mudurnu Valley earthquake ruptured a southern trace. After the 1999 earthquakes, Parson's et al. (2000), using the same methodology as Stein et al. (1997), calculated that the fault zone in the Marmara region experienced an increase in stress, and considering the absence of recent earthquakes there, suggest that it is the next to fail.

The historical record of earthquakes for this region is rich. In addition to the aforementioned earthquakes this century, a M7 event in 1894 also did damage to Istanbul and was believed to be centered in the eastern Marmara Sea region. Another event in 1878 may have occurred farther east, possibly in the Izmit to Sapanca section of the fault. Other than these, one must go back to a sequence in the 18<sup>th</sup> century for the truly large events to have struck the region. A very large event struck the central segments of the NAF in 1668, followed by the M7.5 1719 earthquake in the Izmit region. This was followed by the M7 1754, also somewhere east of the Marmara Sea, and the M7.6 April 1766 event within the Marmara. Three months later, the M7.6 August 1766 earthquake ruptured the Galipoli segment along the Saros-Ganos fault. It appears, then, that the previous sequence, which occurred over a period of nearly 100 years, ruptured at least the entire western half of the fault zone. Based on our paleoseismic work, seismic slip in these events was high, similar to that in the 1999 earthquakes.

The Marmara Sea region, in contrast, has not sustained significant rupture since the 1766 earthquake. Considering that the entire fault to the east and west has ruptured this century with  $\pm 4$  m of slip, and considering that the 1999 earthquakes increased the state of stress along the fault zone in the Marmara region, failure of the fault near Istanbul is probably imminent.

## References Cited

- Ambraseys, N.N. and Finkel, C.F., 1987a, The Saros-Marmara earthquake of 9 August, 1912. *Earthquake Engineering and Structural Dynamics*, v. 15, 189-211.
- Ambraseys, N.N. and Finkel, C.F., 1987b, Seismicity of Turkey and neighboring regions, 1899-1915, *Annales Geophys.*, v. 5B, p. 701-726.
- Ambraseys, N.N. and Finkel, C.F., 1991, Long-term seismicity of Istanbul and the Marmara Sea region: *Terra Nova*, v. 3, p. 527-539.
- Ambraseys, N.N. and Finkel, C.F., 1995, *The Seismicity of Turkey and Adjacent Areas, A Historical Review, 1500-1800*. M.S. EREN, Istanbul, 240 p.
- Barka, A.A., 1992, The North Anatolian fault zone: *Annales Tectonicae*, v. 6, p. 164-195.
- Parsons, T., Barka, A., Toda, S., Stein, R., and Dietrich, J.H., 2000, Influence of the 17 August 1999 earthquake on seismic hazards in Istanbul: in *The 1999 Izmit and Duzce Earthquakes: Preliminary Results* (A. Barka, O. Kozaci, S. Akyuz, and E. Altunel, editors), Istanbul Technical University. 295-310.
- Reilinger, R.E., McClusky, S.C., Oral, M.B., King, R.W., Toksoz, M.N., Barka, A.A., Kinik, I., Lenk, O., and Sanli, I., 1997, Global positioning system measurements of present-day crustal movements in the Arabian-African-Eurasian plate collision zone: *J. Geophys. Res.*, v.102, p. 9983-9999.
- Rockwell, T., A. Barka, T. Dawson, K. Thorup, and S. Akyuz, 2001, Paleoseismology of the Gazikoy-Saros segment of the North Anatolia fault, northwestern Turkey: Comparison of the historical and paleoseismic records, implications of regional seismic hazard, and models of earthquake recurrence: *Journal of Seismology*, V. 5, No. 3, p. 433-448.
- Rockwell, T.K., S. Lindvall, T. Dawson, R. Langridge, W. Lettis, and Y. Klinger, 2002, Lateral offsets on surveyed cultural features resulting from the 1999 Izmit and Duzce earthquakes, Turkey: *Bulletin of the Seismological Society of America*, v. 92, v.1.
- Sieh, Kerry, 1996, The repetition of large-earthquake ruptures, *Proc. Nat. Acad. Sci.*, v. 93, pp. 3764-3771.

Straub, C. and Kahle, H., 1995, Active crustal deformation in the Marmara Sea region, NW Anatolia, inferred from GPS measurements: *Geophysical Research Letters*, v. 22, no. 18, pp. 2533-2536.

Straub, C.S., 1996, Recent crustal deformation and strain accumulation in the Marmara Sea region, N.W. Anatolia, inferred from GPS measurements. unpub. Ph.D. dissertation, Swiss Federal Institute of Technology at Zurich, 122 p. plus appendices.